MAGNETIC PROPERTIES OF YAMATO-7301(j), -7305 (k) AND -7304 (m) CHONDRITES IN COMPARISON WITH THEIR MINERALOGICAL AND CHEMICAL COMPOSITIONS

Takesi NAGATA

National Institute of Polar Research, Kaga 1-chome, Itabashi-ku, Tokyo 173

Abstract: Magnetic properties, represented by the magnetic hysteresis curves at room temperature and the thermomagnetic curves, of Yamato-7301(j), -7305(k), and -7304(m) chondrites are compared with their chemical and petrographic compositions.

Yamato (j) chondrite (H4) contains a metallic phase of 8.0 wt% comprising kamacite of 5.3 wt%Ni and smaller amounts of plessite and taenite, accompanied by non-magnetic metallic oxides. It seems very likely that the metallic oxides were in the form of hydroxides in the original state and were transformed to substituted magnetites by a heating. The metallic phase has been much oxidized by severe weathering.

Yamato (k) chondrite (L5) contains a metallic phase of 8.6 wt% comprising kamacite of 6.5 wt% Ni and α_2-phase of (13–25) wt% Ni, suggesting that this chondrite was reheated to about 1000°C and rapidly cooled to result in a production of α_2-phase.

Yamato (m) chondrite (L5) contains a metallic phase of 8.3 wt% comprising kamacite of 5.5 wt% Ni and taenite, suggesting that this chondrite was almost equilibrated because of its very slow cooling and no appreciable effect of later metamorphism.

Tables 3 and 4 give their basic magnetic properties, and Table 2 their chemical compositions.

1. Introduction—Petrographic and Chemical Compositions

Petrographic and mineral compositions of Yamato-7301 (j), -7305 (k) and -7304 (m) chondrites have been examined in fair detail by YAGI *et al.* (1978). Model mineralogical compositions obtained by the workers are summarized in Table 1. As shown in the table, all the three meteorites contain 12–14 vol.% of chondrules, and the mineralogical compositions of olivines and pyroxenes and other minerals in these chondrites indicate that Yamato (j), (k) and (m) chondrites can be identified to H4, L5 and L5 chondrites respectively. Yamato (j) chondrite, however, contains a considerable amount of reddish brown oxidized products of metallic and sulfide phases in its matrix. These oxidized products are present around iron-nickel and troilite grains, suggesting that this chondrite has been sub-

jected to a severe weathering effect.

The bulk chemical compositions of the three chondrites have been determined by YAGI *et al.* (1978) also, the result being summarized in Table 2. It is clearly indicated in the chemical data too that Yamato (j) chondrite contains unusually large amounts of NiO, CoO and H_2O, suggesting that this chondrite has been considerably oxidized. Comparing the chemical composition of Yamato (j) H-chondrite with that of Yamato (k) and (m) L-chondrites, it may be observed in Table 2 that the FeO content is considerably larger and the FeS content is considerably smaller in Yamato (j) than those in Yamato (k) and (m), and that the metallic Fe and Ni contents are approximately the same in the three chondritic meteorites. These chemical data also may suggest that the metal and sulfide phases of Yamato (j) have been much oxidized, resulting in an increase in the FeO content and a decrease in the Fe and FeS contents. One of the problems examined in the present study is how the mineralogical and chemical characteristics of these three chondrites are reflected in their magnetic properties, in particular, in connection with possible effects of weathering on Yamato (j) H-chondrite. Another problem will be an appreciably large difference of the content of opaque phase in Yamato (k) and (m) chondrites between the petrographic data and the chemical ones. As far

Table 1. Model mineralogical compositions of Yamato (j), (k) and (m) chondrites.

Minerals	Yamato (j) (H4)	Yamato (k) (L5) (vol. %)	Yamato (m) (L5)
(Matrix)			
Olivine	45.34	42.97	45.68
Orthopyroxene	16.66	26.28	18.51
Clinopyroxene	2.81	1.80	1.11
Plagioclase	3.24	6.42	5.66
Opaque phase	10.00	8.13	14.74
Other*	9.65	0.00	0.00
(sub-total)	(87.7)	(85.6)	(85.7)
(Chondrule)			
Olivine	6.92	5.72	6.61
Orthopyroxene	3.75	6.76	5.38
Clinopyroxene	0.81	0.88	0.61
Plagioclase	0.52	0.58	0.93
Opaque phase	0.30	0.46	0.77
(sub-total)	(12.3)	(14.4)	(14.3)
Total	100.0	100.0	100.0

* Reddish brown oxidized products of metallic and sulfide phases.

(after YAGI *et al.*, 1978)

Table 2. Chemical composition of Yamato (j), (k) and (m) chondrites.

	Yamato (j) (H)	Yamato (k) (L5) (wt %)	Yamato (m) (L5)
(Silicate phase)			
SiO_2	35.98	39.15	39.38
MgO	23.30	24.52	24.60
FeO	18.92	13.10	13.02
Al_2O_3	1.88	2.08	2.16
CaO	1.66	1.83	1.79
Na_2O	1.01	1.05	1.00
K_2O	0.12	0.13	0.13
Cr_2O_3	0.60	0.31	0.41
MnO	0.35	0.38	0.38
TiO_2	0.10	0.11	0.10
P_2O_5	0.25	0.27	0.27
H_2O	1.24	—	—
CO_2	0.35	—	—
NiO	0.88	—	—
CoO	0.05	—	—
(Metal phase)			
Fe	7.21	7.64	7.50
Ni	0.77	0.96	0.83
Co	0.05	0.06	0.06
(Sulfide phase)			
FeS	5.05	7.57	8.44
NiS	0.29	0.06	0.03
Total	100.06	99.09	100.10

(after YAGI *et al.*, 1978)

as the chemical compositions given in Table 2 are concerned, Yamato (m) is not appreciably different from Yamato (k); namely, the silicate phase compositions are approximately the same in the two L-chondrites, and the content of metallic phase comprising Fe, Ni and Co and that of FeS+NiS amount to 8.66 and 7.63 wt% respectively in Yamato (k) and to 8.39 and 8.47 wt% respectively in Yamato (m). In the mineralogical compositions shown in Table 1, however, the total contents of opaque phase in Yamato (k) and (m) amount to 8.6 and 15.5 vol.% respectively. Since the magnetic analysis should be able to reasonably well identify the composition and structure of metallic phase in meteorites, magnetic studies of these two L-chondrites in comparison with their petrographic and chemical compositions may contribute to the understanding of their composition, structures and thermal

histories.

2. Magnetic Properties

The basic magnetic parameters of the three chondrites observed at room temperature are summarized in Table 3. In this table, a ratio of saturation magnetization (I_s) to the chemically estimated total content of metals (Fe°+Ni°+Co°) also is given for each sample. The ratio I_s/(Fe°+Ni°+Co°) theoretically represents the average specific intensity of saturation magnetization ($I_s°$) of metallic phase, if the magnetization of oxidized or sulfide ferromagnetic (or ferrimagnetic) minerals is negligibly small. The ratio for Yamato (j) and (m) chondrites is close to 200 emu/gm, which is a reasonable value of native irons in meteorites, which comprise mostly α-phase and partly γ-phase or $(\alpha+\gamma)$-phase of Fe–Ni–Co–P alloy. However, the observed value of I_s/(Fe°+Ni°+Co°) of Yamato (k) chondrite is considerably smaller than the specific saturation magnetization of native irons. The discrepancy could be attributed to either presence of a considerable amount of low Ni γ-phase ($\lesssim$25 wt% Ni) whose Curie point is lower than room temperature or some errors in either or both chemical and magnetic analyses.

Ratios χ_0/I_s, I_R/I_s and I_R/χ_0 given in Table 3 are theoretically expressed as

$$\chi_0/I_s \simeq 1/(NJ_s), \tag{1}$$

$$I_R/I_s \simeq H_c/(NJ_s), \tag{2}$$

Table 3. Magnetic properties of Yamato (j), (k) and (m) chondrites.

Magnetic parameters	Yamato			Unit
	j(H4)	k(L5)	m(L5)	
Magnetic susceptibility χ_0 (20°C)	7.0×10^{-3}	4.1×10^{-3}	4.5×10^{-3}	emu/gm/Oe
Saturation magnetization I_s (20°C)	15.0	14.3	16.6	emu/gm
Saturation remanence I_R (20°C)	0.14	0.045	0.024	〃
Coercive force H_c (20°C)	16	8	4	Oersteds
Remanence coercive force H_{Rc} (20°C)	1,700	375	175	〃
χ_0/I_s	4.6×10^{-4}	2.9×10^{-4}	2.7×10^{-4}	(Oersted)$^{-1}$
I_R/I_s	9.2×10^{-3}	3.1×10^{-3}	1.5×10^{-3}	
I_R/χ_0	20	11	5	Oersted
I_s/(Fe^0+Ni^0+Co^0)	191	165	198	emu/gm

$$I_R/\chi_0 \simeq H_c, \tag{3}$$

where J_s and N denote respectively the average saturation magnetization of ferromagnetic constituents (per cc) and the average value of demagnetizing factor of ferromagnetic grains. As already discussed (NAGATA *et al.*, 1975), the numerical value of $(NJ_s)^{-1}$ for ordinary chondrites should be about 2×10^{-4} (Oersted)$^{-1}$, if the ferromagnetic grains comprise mostly FeNi metals of α-phase (*i.e.* $J_s=(1.5$–$1.7)\times10^3$ emu/cc) having moderate grain shapes ($N=3$–4). The observed values of χ_0/I_s of the three chondrites are a little larger than the theoretically expected value of $(NJ_s)^{-1}$, but their order of magnitude is same as that of the theoretical expectation. In the case of lunar materials, in which also the ferromagnetic constituents are native irons, the observed values of χ_0/I_s ranges from 5×10^{-4} to 1×10^{-2}, indicating that the major parts of χ_0 are due to the superparamagnetic susceptibility of very fine grains of native iron (NAGATA *et al.*, 1973). It may be concluded from the present and previous (NAGATA *et al.*, 1975) studies, therefore, that the relative content of superparamagnetically fine grains of native iron in chondrites is much smaller than that in lunar materials. Thus, ratio I_R/χ_0 derived from the observed values of I_R and χ_0 is approximately the same as the directly observed value of H_c for the three chondrites.

The thermomagnetic curves of the three chondrites are shown in Figs. 1, 3 and 5, where the first and second run measurements are separately illustrated.

2.1. *Yamato* (*j*)

A kamacite phase which has $\Theta_{\alpha\to\gamma}$ transition temperature at 755°C and $\Theta_{\gamma\to\alpha}$ transition temperature at about 660°C is stable and reproducible throughout the first and second run measurements. The average Ni-content of the kamacite phase is evaluated from $\Theta_{\alpha\to\gamma}$ and $\Theta_{\gamma\to\alpha}$ temperatures to be about 5.3 wt%. A magnetic phase which has a transition point at 577°C in the first heating process may be identified to a plessite ($\alpha+\gamma$)-phase, which is irreversibly transformed into a taenite (γ)-phase after heating beyond 577°C. The newly produced γ-phase appears as an additional magnetization below about 350°C in the first cooling curve. However, a magnetic phase which has a transition temperature at about 575°C still remains in the first cooling curve and the heating and cooling curves in the second-run measurement. This magnetic phase may be identified to a magnetite (or a substituted magnetite)-phase which is produced by the heating as will be discussed later in more detail in comparison with chemical and mineralogical data of this chondrite. Summarizing these probable interpretations of the magnetic phases, the heating and cooling thermomagnetic curves in the first and second runs, shown in Fig. 1, may be interpreted to be composed of several different magnetic phases as illustrated in Fig. 2. Namely, a kamacite phase of about 5.3 wt% Ni is a stable component; a plessite phase shown by a heating plessite component (I) is transformed into a taenite phase represented by a cooling taenite component which

is identical with a heating taenite component (II), where this component is a sum of the newly produced taenite phase and the initially existing taenite which is given by a heating taenite component (I); a magnetite phase newly produced by the first heating is represented by a cooling magnetite+plessite component (I) which is approximately equal to the heating and cooling magnetite+plessite component (II). It seems, however, that a cooling magnetite+plessite component (I) still contains a small amount of coarse plessite grains which are transformed into

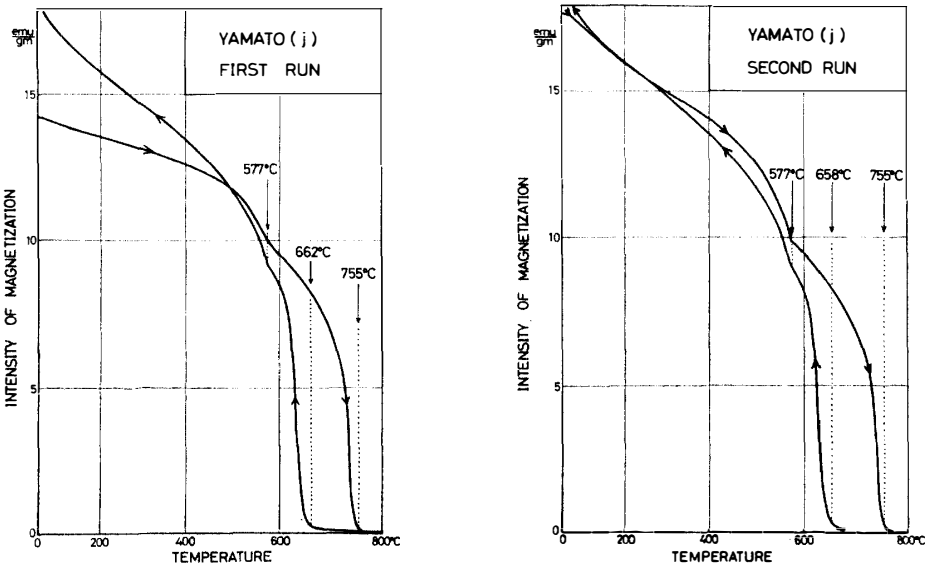

a. First run. *b. Second run.*

Fig. 1. Thermomagnetic curves of Yamato (j) chondrite.

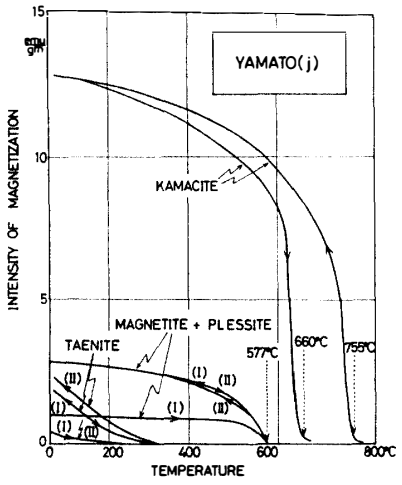

Fig. 2. Interpretation of thermomagnetic curves of Yamato (j) chondrite.

taenites by the second heating, resulting in an increase of taenite component as represented by a cooling taenite curve (II).

The initial (before the first heating) and final (after the second cooling) magnetic compositions of this chondrite may therefore be summarized as follows:

Initial composition				Final composition			
Kamacite:	$I(\alpha)$	=13.3	emu/gm	Kamacite:	$I(\alpha)$	=13.3	emu/gm.
Plessite:	$I(\alpha+\gamma)$	= 1.6	〃	Magnetite:	$I(Mt)$	= 2.9	〃
Taenite:	$I(\gamma)$	= 0.4	〃	Taenite:	$I(\gamma)$	= 3.0	〃
Total:	I_s	=15.3	〃	Total:	I_s	=19.2	〃

2.2. Yamato (k)

As shown in Fig. 3, the second-run thermomagnetic curves are almost the same as the first-run ones for this chondrite. A magnetic phase which has $\Theta_{\alpha\to\gamma}$ temperature at 740°C and $\Theta_{\gamma\to\alpha}$ temperature at about 625°C may be identified to a kamacite of 6.5 wt% Ni. The other stable magnetic phase of $\Theta_{\alpha\to\gamma}$=655°C and $\Theta_{\gamma\to\alpha}$=405°C may be identified to an α_2-phase of about 13 wt% Ni. Since the temperature gradient of magnetization of the α_2-phase component is considerably smaller than that of a single α_2-phase of 13 wt% Ni, it seems that the distribution spectrum of the Ni-content in the α_2-phase grains is extended over a certain broad range extending toward higher-Ni-contents. With the aid of an already known method of analysis (NAGATA *et al.*, 1974), the Ni-content spectrum in the metallic phase of Yamato (k) chondrite has been obtained as illustrated in Fig. 4. As clearly shown in this figure, the Ni-content spectrum comprises a sharp line spectrum of α-phase of about 6.5 wt% Ni and a broad continuous spectrum of α_2-phase ranging from 12 wt% Ni to about 25 wt% Ni with a maximum peak around 13 wt% Ni. This result strongly suggests that a larger portion of metallic grains

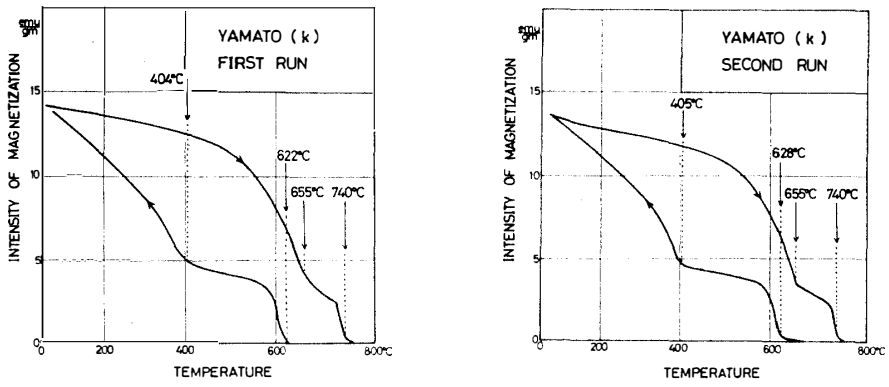

a. First run. *b. Second run.*

Fig. 3. Thermomagnetic curves of Yamato (k) chondrite.

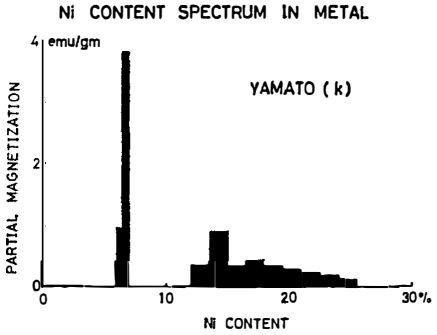

Fig. 4. Ni-content spectrum in metallic phase in Yamato (k) chondrite derived from magnetic analysis.

in this chondrite was reheated up to a temperature of γ-phase domain of the Fe–Ni–P–Co phase equilibrium diagram and then rapidly cooled down to result in a diffusionless transformation to an α_2-phase.

Summarizing these experimental results, the magnetic composition of this chondrite may be represented by the following stable two components, namely,

Initial and final compositions

Kamacite:	$I(\alpha)$	= 5.0 emu/gm
α_2-phase:	$I(\alpha_2)$	= 9.3 〃
Total:	I_s	=14.3 〃 .

2.3. *Yamato (m)*

As shown in Fig. 5, the second-run thermomagnetic curves are approximately

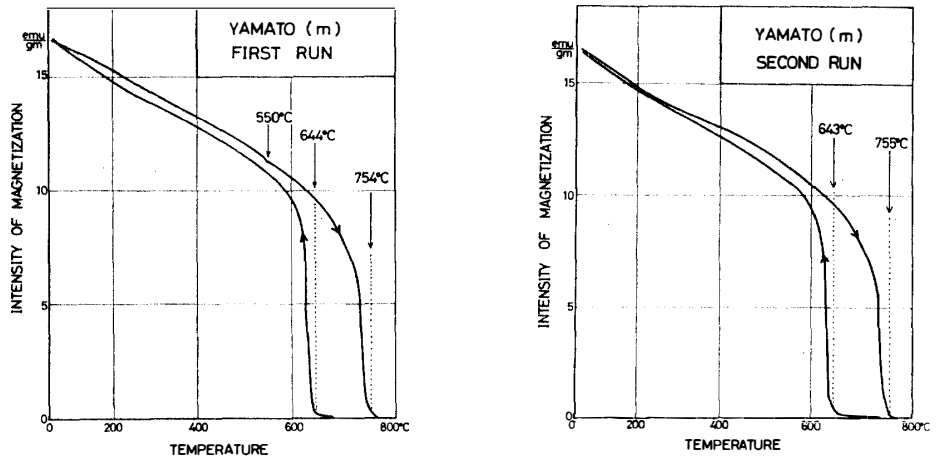

a. First run. *b. Second run.*

Fig. 5. Thermomagnetic curves of Yamato (m) chondrite.

identical with the first-run ones for this chondrite. It seems likely, however, that the first heating curve contains a small amount of plessite phase which has its transition temperature at about 550°C, and has been transformed into a taenite phase after the first heating. A stable magnetic component of $\Theta^*_{\alpha\to\gamma}$=755°C and $\Theta^*_{\gamma\to\alpha}$=644°C can be identified to a kamacite phase of 5.5 wt% Ni. Comparing the first heating curve with the second heating one, the room temperature intensity of plessite phase can be estimated to be approximately 0.3 emu/gm. In addition, a taenite phase having its maximum Curie point at about 500°C can be clearly observed. The second-run thermomagnetic curves consist of kamacite phase and taenite one only. The magnetic composition of this chondrite may therefore be represented by

Initial composition			Final composition		
Kamacite:	$I(\alpha)$	=14.1 emu/gm	Kamacite:	$I(\alpha)$	=14.1 emu/gm
Plessite:	$I(\alpha+\gamma)$	= 0.3 〃	Taenite:	$I(\gamma)$	= 2.5 〃
Taenite:	$I(\gamma)$	= 2.2 〃			
Total:	I_s	=16.6 〃	Total:	I_s	=16.6 〃 .

The magnetic transition temperatures of the three chondrites are summarized in Table 4, where the thermomagnetic characteristics of taenite phase are not included because the composition of individual taenite phases is too much complicated to be simply expressed.

Table 4. Thermomagnetic characteristics of Yamato (j), (k) and (m) chondrites.

Magnetic transition temperature	Yamato		
	j(H4)	k(L5)	m(L5)
(First-run measurement)			
$\Theta^*_{\alpha\to\gamma}$	755	740	754°C
$\Theta^*_{\gamma\to\alpha}$	662	622	644°C
$\Theta^*_{\alpha_2\to\gamma}$	—	655°C	—
$\Theta^*_{\gamma\to\alpha_2}$	—	404°C	—
$\Theta^*_{(\alpha+\gamma)\to\gamma}$	577	—	550°C
(Second-run measurement)			
$\Theta^*_{\alpha\to\gamma}$	755	740	755°C
$\Theta^*_{\gamma\to\alpha}$	658	628	643°C
$\Theta^*_{\alpha_2\to\gamma}$	—	655°C	—
$\Theta^*_{\gamma\to\alpha_2}$	—	405°C	—
$\Theta(Mt)$	575°C	—	—

3. Comparison of Magnetic Composition with Chemical and Mineralogical Compositions

For Yamato (j), (k) and (m) chondrites, the magnetic composition is estimated in fair detail in the present study, in addition to their chemical and mineralogical compositions obtained by YAGI *et al.* (1978). It will be desirable therefore to examine the mutual relationship, as quantitatively as possible, among the three different kinds of experimental data on the opaque phase in these chondrites.

3.1. Yamato (j)

The initial magnetic composition at room temperature of this chondrite is represented by $I(\alpha)=13.3$, $I(\alpha+\gamma)=1.6$ and $I(\gamma)=0.4$ emu/gm, while the chemical composition of metallic phase by $m(\mathrm{Fe})=7.21$, $m(\mathrm{Ni})=0.77$ and $m(\mathrm{Co})=0.05$ wt%. Since the saturation magnetizations of 5.3 wt% kamacite and a model taenite (in which the average Ni-content is 30.9 wt%: See Appendix) are given by $I_s^\circ(\alpha)=218$ emu/gm and $I_s^\circ(\gamma)=155$ emu/gm respectively, the weight percentages of α- and γ-phases and Fe- and Ni-components in respective phases are estimated as,

$m(\alpha)=6.11$; $m_\alpha(\mathrm{Fe})=5.79$, $m_\alpha(\mathrm{Ni})=0.32$ (wt%),
$m(\gamma)=0.26$; $m_\gamma(\mathrm{Fe})=0.18$, $m_\gamma(\mathrm{Ni})=0.08$ (wt%).

Since $m(\mathrm{Fe})=7.21$ and $m(\mathrm{Ni})=0.77$ wt% respectively, Fe and Ni percentages in the remaining $(\alpha+\gamma)$-phase and the resultant content of $(\alpha+\gamma)$-phase are to be estimated as

$m(\alpha+\gamma)=1.61$; $m_{\alpha+\gamma}(\mathrm{Fe})=1.24$, $m_{\alpha+\gamma}(\mathrm{Ni})=0.37$ (wt%).

Then, the average Ni-content in this $(\alpha+\gamma)$-phase is to be about 23 wt%. Then, the observed magnetization of $(\alpha+\gamma)$-phase is considered to be due to that of α-component only, because Curie-point of taenite of about 23 wt% Ni is below 0°C. As the saturation magnetization of α-phase of 23 wt% Ni is about 185 emu/gm, the weight percent of α-component in $m(\alpha+\gamma)$ is evaluated as $m_{\alpha+\gamma}(\alpha)=0.85$ wt%, and therefore $m_{\alpha+\gamma}(\gamma)=0.76$ wt%. This result may suggest that an expected separation of α_2-phase into α- and γ-phases in the $(\alpha+\gamma)$-structure is still in its early stage in this chondrite. Summarizing these interpretations of the three metallic phases, no essential conflict can be pointed out between the magnetic and chemical compositions.

The final stage magnetic composition is represented by $I(\alpha)=13.3$, $I(\gamma)=3.0$ and $I(Mt)=2.9$ emu/gm. Namely, α-phase is kept unchanged, but the $(\alpha+\gamma)$-phase has been transformed into a γ-phase and a magnetite phase has been newly produced. As far as the mass conservation of metallic phases is concerned, therefore, the weight percentage of α- and γ-phases in this stage should be given by $m(\alpha)=6.11$ and $m(\gamma)=1.87$ wt% repsectively. If the magnetization of γ-phase could be represented by that of the model γ-phase, the magnetization of γ-phase is evaluated as

2.9 emu/gm, which is close to the observed value. However, the γ-phase in the present interpretation on the basis of chemical analysis data is a mixture of $m(\gamma_1)=0.26$ wt% of 30.9% in average Ni-content (Model γ-phase) and $m(\gamma_2)=1.61$ wt% of 23% Ni γ-phase. In other words, the present interpretation of the magnetic composition theoretically requires that the Ni-content in the metallic phase is larger by 0.11% than the value obtained in the chemical analysis. In the present interpretation, however, the presence of Co and a possible effect of P of a small amount are ignored.

It is experimentally ascertained that the final stage magnetic composition contains a thermally reversible and reproducible ferromagnetic phase which can be almost certainly identified to a magnetite or a substituted magnetite phase. Since the initial magnetic composition does not contain the corresponding magnetic phase and the original chemical composition contains considerable amounts of H_2O, NiO and CoO, it seems very likely that the original mineral composition contains non-magnetic hydroxides of metals such as $Fe(OH)_2$, $Ni(OH)_2$, $Co(OH)_2$ and $Fe(OH)_3$. Probably, these metallic hydroxides are in their solid solution stages, because they are considered as the hydroxidation products of metallic (Fe, Ni, Co) alloys and troilite phase of (Fe, Ni, Co)S. Then, the dehydration process by heating in a practically vacuum space may result in the following chemical reactions to produce magnetite and substituted magnetites; namely,

$$\begin{aligned} &Fe(OH)_2 \longrightarrow FeO+H_2O, && FeO+Fe_2O_3=Fe_3O_4,\\ &Ni(OH)_2 \longrightarrow NiO+H_2O, && NiO+Fe_2O_3=Fe_2NiO_4,\\ &Co(OH)_2 \longrightarrow CoO+H_2O, && CoO+Fe_2O_3=Fe_2CoO_4,\\ &2Fe(OH)_3 \longrightarrow Fe_2O_3+3H_2O, \end{aligned}$$

where the final products, Fe_3O_4, Fe_2NiO_4 and Fe_2CoO_4 are probably in their solid solution state.

In considering the above mentioned possible processes of producing magnetite and substituted magnetites from the original metallic hydroxides, it is reasonable to assume that all parts of NiO and CoO form $Ni(OH)_2$ and $Co(OH)_2$ respectively with the corresponding amounts of H_2O and the remaining parts of H_2O form $Fe(OH)_3$ and $Fe(OH)_2$ with FeO in the chemical composition given in Table 2 so that the chemical reaction chains under consideration can be quantitatively satisfied.

On these assumptions, the weight contents of metallic hydroxides in the initial state are estimated as

$m[Ni(OH)_2]=1.092\%$, $m[Co(OH)_2]=0.062\%$, $m[Fe(OH)_2]=0.429\%$ and $m[Fe(OH)_3]=3.681\%$,

and the final dehydrated state as

$m[Fe_3O_4]=1.106\%$, $m(Fe_2NiO_4)=2.761\%$, $m(Fe_2CoO_4)=0.157\%$.

Since the saturation magnetizations of Fe_3O_4, Fe_2NiO_4 and Fe_2CoO_4 are 98.2,

53 and 94 emu/gm respectively, the total magnetization intensity of the final product of ferrimagnetic solid solution is estimated as

$$I(Mt)=I(Fe_3O_4)+I(Fe_2NiO_4)+I(Fe_2CoO_4)=2.7 \text{ emu/gm}.$$

Summarizing all these interpretations, magnetic, chemical and mineralogical compositions of magnetic components in Yamato (j) chondrite may be expressed as given in Table 5.

Table 5. Magnetic compositions in Yamato (j) chondrite.

(Initial state)					(Final state)			
Metal	wt%	I(emu/gm) (calc.)	I(emu/gm) (obs.)		Metal	wt%	I(emu/gm) (calc.)	I(emu/gm) (obs.)
(5.3%Ni)	6.11	13.3	13.3	⟶	α	6.11	13.3	13.3
γ	0.26	0.4	0.4	⟶	γ	0.26	0.4 } 2.9	3.0
$\alpha+\gamma$	1.61	1.6	1.6	⟶	γ	1.61	2.5 (?) }	
(Involved metallic element; Fe: 7.21%, Ni: 0.77%)								
Hydroxide	wt%	I(emu/gm) (calc.)	I(emu/gm) (obs.)		Metal	wt%	I(emu/gm) (calc.)	I(emu/gm) (obs.)
$Ni(OH)_2$	1.09	0	0	⟶	Fe_2NiO_4	2.76	1.46	
$Co(OH)_2$	0.06	0	0	⟶	Fe_2CoO_4	0.16	0.15 } 2.7	2.9
$Fe(OH)_2$	0.43	0	0	⟶	Fe_3O_4	1.11	1.09	
$Fe(OH)_3$	3.68	0	0					
(Involved oxide; H_2O: 1.24%, NiO: 0.88%, CoO: 0.05%, FeO: 2.82%)								

3.2. *Yamato (k)*

The magnetic composition at room temperature of this chondrite is represented by $I(\alpha)=5.0$ emu/gm and $I(\alpha_2)=9.3$ emu/gm throughout the first and second run examinations, while its chemical composition of metallic phase by $m(\text{Fe})=7.64$, $m(\text{Ni})=0.96$ and $m(\text{Co})=0.06$ wt%.

As briefly discussed in Section 2, the observed total magnetization of this chondrite is considerably smaller than its theoretical estimate on the basis of Fe- and Ni-contents determined by a chemical analysis. In the result of magnetic analysis shown in Fig. 4, the total weight content and magnetization of α-phase (6.0–7.0 wt%Ni) are $m(\alpha)=2.36\%$ and 4.96 emu/gm respectively, while those of α_2-phase (12.0–25.5 wt%Ni) are 4.44% and 9.34 emu/gm respectively. From these magnetic data, the total weight contents of metallic Fe and Ni are estimated as

$m(\mathrm{Fe})=m_{\alpha}(\mathrm{Fe})+m_{\alpha_2}(\mathrm{Fe})=5.96\%$ and $m(\mathrm{Ni})=m_{\alpha}(\mathrm{Ni})+m_{\alpha_2}(\mathrm{Ni})=0.84\%$ respectively, and consequently the total metal content should be $m(\mathrm{metal})=6.80$ wt%. This magnetic estimate of total metal content is considerably smaller than its chemically obtained value, 8.66 wt%.

If both chemical and magnetic data are correct, there must be a non-magnetic metallic phase of 1.80 wt% which comprises 1.68% of Fe and 0.12% of Ni, where the presence of 0.06% of Co is ignored. Then, the Ni-content in the expected non-magnetic metallic phase is to be 6.6 wt%, which is within the range of ferromagnetic α-phase. This result may suggest that a chemically analyzed specimen contains $m(\alpha)=4.16\%$ of 6.5%Ni α-phase and $m(\alpha_2)=4.44\%$ of α_2-phase. Thus, the most plausible explanation of the discrepancy between the magnetic and chemical analyses of metallic phase could be such that the magnetically analyzed part (0.125 gm) contains a less amount of α-phase compared with that in the chemically analyzed one, because of a little inhomogeneity of distribution of metallic grains within this chondrite.

Another plausible interpretation would be such that some possible experimental or analysis errors are present either in the magnetic analysis of the Ni-content spectra or in the chemical analysis. If we assume that the total sum of Ni abundance in α_2-phase is 0.14% less than that estimated on the basis of the Ni-content spectrum of α_2-phase, given by the magnetic analysis, co-existence of γ-phase of 13 wt%Ni could be expected. This interpretation appears to be metallographically reasonable: The metallic phase of $m=8.64\%$ in molten condition in the Fe–Ni–P system is represented by 11.2%: At about 630°C in the slow cooling process, the metal phase is to be separated into an α-phase of about 6.5 wt%Ni and a γ-phase or an $(\alpha+\gamma)$-phase of about 13% where $m(\alpha)=2.36$ wt% and $m(\gamma)$ or $m(\alpha+\gamma)=6.24$ wt%. By reheating and succeeding rapid cooling, a part of the γ- or $(\alpha+\gamma)$-phase may have become α_2-phase of $m(\alpha_2)=4.44$ wt% by the diffusionless transformation mechanism, the remaining portion of $m(\gamma)=1.80$ wt% being kept in γ-phase. As Curie point of 13%Ni γ-phase is far below 0°C, its magnetization is practically zero at room temperature.

Summarizing these interpretations, magnetic, chemical and mineralogical com-

Table 6. Magnetic composition in Yamato (k) chondrite.

Metal	wt%	I(emu/gm) (calc.)	I(emu/gm) (obs.)
α(6.5%Ni)	2.36	5.0	5.0
α_2(13~25%Ni)	4.44	9.3	9.3
γ(13%Ni)?	1.80	0	0

(Involved metallic element; Fe: 7.64%, Ni: 0.96%)

positions of metallic component in Yamato (k) chondrite may be expressed as given in Table 6.

3.3. *Yamato (m)*

The initial magnetic composition at room temperature of this chondrite is represented by $I(\alpha)=14.1$, $I(\alpha+\gamma)=0.3$ and $I(\gamma)=2.2$ emu/gm, and the final one by $I(\alpha)=14.1$ and $I(\gamma)=2.5$ emu/gm, while its chemical composition of metallic phase by $m(\mathrm{Fe})=7.50$, $m(\mathrm{Ni})=0.83$ and $m(\mathrm{Co})=0.06\%$.

From α- and γ-phases in the initial magnetic composition, Fe- and Ni-contents in these phases are estimated as

$$m(\alpha)=6.56;\quad m_\alpha(\mathrm{Fe})=6.20,\quad m_\alpha(\mathrm{Ni})=0.36\ (\mathrm{wt}\%),$$
$$m(\gamma)=1.42;\quad m_\gamma(\mathrm{Fe})=0.99,\quad m_\gamma(\mathrm{Ni})=0.43\ (\mathrm{wt}\%).$$

Subtracting $m_\alpha(\mathrm{Fe})$ and $m_\gamma(\mathrm{Fe})$ from $m(\mathrm{Fe})$, and also $m_\alpha(\mathrm{Ni})$ and $m_\gamma(\mathrm{Ni})$ from $m(\mathrm{Ni})$, the distribution of Fe and Ni in the remaining $(\alpha+\gamma)$-phase and the resultant content of $(\alpha+\gamma)$-phase are estimated as $m(\alpha+\gamma)=0.35$; $m_{\alpha+\gamma}(\mathrm{Fe})=0.31$, $m_{\alpha+\gamma}(\mathrm{Ni})=0.043$ (wt%). This result may suggest that the average Ni-content in $(\alpha+\gamma)$-phase is about 12%, and consequently $I(\alpha+\gamma)=0.3$ emu/gm corresponds to $m_{\alpha+\gamma}(\alpha)\simeq 0.14\%$. It does not seem, however, that the present magnetic analysis is sufficiently precise to quantitatively deal with the composition of $(\alpha+\gamma)$-phase which is only a small part of the total metallic phase.

The final magnetic composition can be similarly represented by

$$m(\alpha)=6.56;\quad m_\alpha(\mathrm{Fe})=6.20,\quad m_\alpha(\mathrm{Ni})=0.36\ (\mathrm{wt}\%),$$
$$m(\gamma)=1.61;\quad m_\gamma(\mathrm{Fe})=1.13,\quad m_\gamma(\mathrm{Ni})=0.48\ (\mathrm{wt}\%),$$

which give $m(\mathrm{Fe})=7.33$ and $m(\mathrm{Ni})=0.84$ wt%. These magnetically estimated values of $m(\mathrm{Fe})$ and $m(\mathrm{Ni})$ are reasonably close to their respective chemically determined ones. Summarizing these interpretations, magnetic, chemical and metallographic compositions of the metallic phase of Yamato (m) chondrite may be expressed as given in Table 7.

Table 7. Magnetic composition in Yamato (m) chondrite.

(Initial state)					(Final state)				
Metal	wt%	I(emu/gm)			Metal	wt%	I(emu/gm)		
		(calc.)	(obs.)				(calc.)		(obs.)
α(5.5%Ni)	6.56	14.1	14.1	⟶	α	6.56	14.1		14.1
γ	1.42	2.2	2.2	⟶	γ	1.42	2.2	2.5	2.5
$\alpha+\beta$	0.35	0.3	0.3	⟶	γ	0.35	0.3		

(Involved metallic element; Fe: 7.50%, Ni: 0.83%)

3.4. Remarks on thermomagnetic data in comparison with chemical data

It seems in general that the composition of ferromagnetic phase estimated by the thermomagnetic analysis is in approximate agreement with chemical data for the three Yamato chondrites. There remain, however, several unsolved problems in the magnetic properties of native irons in meteorites which must be clarified in order to make the proposed magnetic analysis more quantitatively reliable.

An unsolved problem will be the thermomagnetic characteristic of $(\alpha+\gamma)$-phase in which Ni-contents in both α- and γ-compositions may be dispersed over a certain range. The ferromagnetization of a fine grained plessite phase generally disappears at a transition temperature ($\Theta^*_{\alpha+\gamma}$) in the first heating thermomagnetic curve, the $(\alpha+\gamma)$-phase being transformed into a γ-phase above this temperature. In the Fe–Ni phase equilibrium diagram or in the Fe–Ni–P one, the transition temperature ($\Theta^*_{\alpha+\gamma}$) represents the transformation from $(\alpha+\gamma)$-phase to γ-phase for the minimum Ni-content portion of plessite. It might be possible, therefore, to analyze the initial thermomagnetic curve of $(\alpha+\gamma)$-phase, $I(\alpha+\gamma)$, by taking into acount both $\Theta^*_{\alpha+\gamma}$-value and the temperature gradient of $I(\alpha+\gamma)$ to evaluate Ni-content spectra in an $(\alpha+\gamma)$-phase.

Another unsolved problem will be the thermomagnetic characteristic of γ-phase which also may comprise a number of components of different Ni-contents. The thermomagnetic characteristics of Fe–Ni alloys in γ-phase dependent on Ni-content have not yet been completely determined, particularly for the low-Ni range. Although a preliminary trial to approximately represent an apparent thermomagnetic property of taenite phase in chondrites by a model γ-phase is made in the present study (see Appendix), the model is still in the stage of a qualitative approximation.

4. Thermal Histories of Individual Chondrites

The average composition of metallic phase of Yamato (m) chondrite is a typical example of almost complete separation into α- and γ-phase caused by a very slow cooling down to about 500°C. On the contrary, the composition of metallic phase of Yamato (k) chondrite is a typical example of reheated native iron, which comprises α- and α_2-phases. Then, from these observed compositions of metallic phase, the thermal histories of these chondrites can be traced to a certain extent, if the metallic phase is simply composed of Fe and Ni only. It has been observed in iron meteorites (*e.g.* GOLDSTEIN and DOAN, 1972), however, that a small content of phosphorus in a Fe–Ni system causes a considerable change in the phase equilibrium diagram of the metallic system, as shown in Fig. 6. Although iron meteorites generally contain phosphorus of an appreciable amount in addition to iron, nickel and cobalt (*e.g.* BUCHWALD, 1975), the content of P in metallic phase of stony meteorites has not been fully examined. In tracing the thermal history of metallic phase in stony meteorites, therefore, a considerable degree of errors may

accompany the temperature determination process.

4.1. Yamato (j)

If the interpretation that the metallic phase in this chondrite was partially hydroxidized by severe weathering, resulting in the presence of NiO, CoO and H_2O in the bulk chemical composition, is accepted, contents of Fe and Ni before the weathering can be evaluated as 9.31 and 1.46 wt% respectively. Assuming then that the molten metallic phase consists of Fe and Ni only, in which m(Ni)/[m(Fe) $+m$(Ni)]=13.6%, the magnetically determined composition of metallic phase as represented by α-phase of 5.3% Ni, ($\alpha+\gamma$)-phase of 23%Ni and γ-phase of about 30%Ni may suggest the thermal history of this chondrite as illustrated in Fig. 6. Namely, this chondrite was very slowly cooled down to about 500°C, approximately keeping the phase equilibrium in the Fe–Ni system. The weathering effect may have taken place after this meteorite fell on the earth's surface.

4.2. Yamato (k)

The Ni-content in the initial molten state of metallic phase in this chondrite is expressed as m(Ni)/[m(Fe)+m(Ni)]=11.2%. The magnetically determined composition of the metallic phase, represented by α-phase of 6.5%Ni and α_2-phase, in which Ni-content is larger than 13%, may suggest the following thermal history of this chondrite as illustrated in Fig. 6. This chondrite was very slowly cooled down

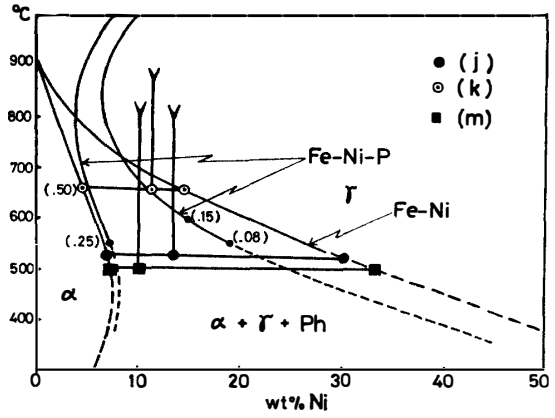

Fig. 6. Phase equilibrium diagrams of Fe–Ni system and Fe–Ni–P system, with probable traces of tharmal history of Yamato (j), (k) and (m) chondrites.

to about 650°C, approximately keeping the phase equilibrium condition, and then cooled a little faster down to about 550°C, precipitating ($\alpha+\gamma$)-phases of (13–25)%Ni; after the formation of this structure, an accident to heat this chondrite up to a temperature of γ-phase domain but below the solidus temperature, (namely about 1000°C) may have happened, and then the entire body was rapidly cooled

down again, resulting in the diffusionless transformations of Ni-rich grains of γ-phase to their α_2-phase and Ni-poor grains to their α-phase.

4.3. Yamato (m)

The metallic phase of Yamato (m) chondrite, in which $m(\mathrm{Ni})/[m(\mathrm{Fe})+m(\mathrm{Ni})] = 10.0\%$, has a comparatively simple composition, *i.e.* α-phase of 5.5%Ni and γ-phase of about 30%Ni. Although a very small amount of $(\alpha+\gamma)$-phase is detectable in its original stage, the major parts of the metal composition suggest that this chondrite was very slowly cooled down to 500°C, keeping the phase equilibrium condition, and a continued slow cooling resulted in the formation of γ-phases whose Ni-content is larger than 30% and the remaining parts of $(\alpha+\gamma)$-phase. The average stage of this cooling process is illustrated in Fig. 6.

4.4. Mutual comparison of thermal histories of the three chondrites

As confirmed in the present study, Yamato (j) and Yamato (k) chondrites were subjected to unusual conditions in their histories; namely, Yamato (j) has been seriously weathered and Yamato (k) was reheated up to about 1000°C, whereas Yamato (m) has been very little metamorphozed after it was very slowly cooled down. As already mentioned, a quantitative tracing of the thermal history of stony meteorites is not fully possible because of ambiguity of the P-content in their metallic phase. As shown in Fig. 6, however, the present qualitative thermal historical interpretation indicates that the abundance of α-phase is much larger than that of γ- and/or $(\alpha+\gamma)$-phase in Yamato (j) and (m) chondrites, whereas α_2-phase is considerably more abundant than α-phase in Yamato (k) chondrite. These results derived from the thermal historical interpretation are in agreement with the magnetically determined compositions of Yamato (j), (m) and (k) chondrites summarized in Tables 5, 7 and 6 respectively.

5. Concluding Remarks

Magnetic characteristics of kamacite phase have been reasonably well clarified so that the content and composition of this α-phase can be well determined from measurements of its thermomagnetic curves. It has been frequently observed (*e.g.* NAGATA and SUGIURA, 1976) in chondritic meteorites, on the other hand, that the plessite phase magnetization disappears or is appreciably reduced at a certain critical temperature by the first heating. As no or very little magnetization of $(\alpha+\gamma)$-phase remains and instead a γ-phase magnetization appears in the succeeding cooling curve, it is certain that the initial $(\alpha+\gamma)$-phase is transformed into a γ-phase at the critical temperature by the heat treatment. In most chondrites, the transformation temperature is between 540°C and 580°C. In reference to the Fe–Ni phase diagram for laboratory time-scale heat treatments, the transformation temperature suggests the minimum Ni-content in $(\alpha+\gamma)$-phase is 22–28 wt% and

the Ni-content spectrum is mostly concentrated near the minimum Ni-content value. The general tendency of the Ni-content spectrum is reflected in the thermomagnetic characteristics of the corresponding transformed γ-phase also. However, magnetic characteristics in detail of $(\alpha+\gamma)$- and γ-phase of Fe–Ni alloy have not yet been well studied for the Ni-content range of <45 wt%. The present study on magnetic behaviors of chondrites in comparison with their chemical compositions is a preliminary trial to understand the composition and structure of these $(\alpha+\gamma)$- and γ-phases in the metallic component of chondrites.

It seems that the observed distinguished differences among the thermomagnetic characteristics of Yamato (j), (k) and (m) chondrites can be qualitatively well interpreted on the basis of the present knowledge of their metallographic compositions and thermal histories. In dealing with these problems more quantitatively, however, a precise knowledge of basic magnetic properties of $(\alpha+\gamma)$- and γ-phases of various compositions has become essentially required. In concluding, therefore, the present study can be regarded as an example of semi-quantitative magnetic analysis of metallographic composition and thermal history of chondritic meteorites.

A part of the thermomagnetic analysis in the present study was carried out with assistance of Dr. N. SUGIURA. The author's sincere thanks are due to him.

References

BOZORTH, R. M. (1951): Ferromagnetism. Amsterdum, Van Nostrand, 1–968.

BUCHWALD, V. F. (1975): Handbook of Iron Meteorites. Berkeley, Univ. California Press, 1418 p.

GOLDSTEIN, J. I. and DOAN, A. S., Jr. (1972): The effect of phosphorus on the formation of the Widmanstätten pattern in the iron meteorites. Geochim. Cosmochim. Acta, **66**, 51–69.

NAGATA, T. (1961) Rock Magnetism. Rev. ed. Tokyo, Maruzen, 1–350.

NAGATA, T., FISHER, R. M. and SCHWERER, F. C. (1974a): Some characteristic magnetic properties of lunar materials. Moon, **9**, 63–77.

NAGATA, T., SUGIURA, N., FISHER, R. M., SCHWERER, F. C., FULLER, M. D. and DUNN, J. R. (1974): Magnetic properties of Apollo 11–17 lunar materials with special reference to effects of meteorite impact. Proc. Fifth Lunar Sci. Conf., 2827–2839 (Geochim. Cosmochim. Acta, Suppl. **5**).

NAGATA, T., SUGIURA, N. and SCHWERER, F. C. (1975): Notes on magnetic properties of the Yamato meteorites. Mem. Natl Inst. Polar Res., Spec. Issue, **5**, 91–110.

NAGATA, T. and SUGIURA, N. (1976): Magnetic characteristics of some Yamato meteorites—Magnetic classification of stone meteorites. Mem. Natl Inst. Polar Res., Ser. C, **10**, 30–58.

YAGI, K., LOVERING, J. F., SHIMA, M. and OKADA, A. (1978): Mineralogical and petrographical studies of the Yamato meteorites, Yamato-7301(j), -7305(k), -7308(l) and -7303(m) from Antarctica. Mem. Natl Inst. Polar Res., Spec. Issue, **8**, 121–141.

(Received May 17, 1978)

Appendix: Thermomagnetic Characteristics of Taenite Phase

In all observed thermomagnetic curves of chondrites, the dependence of magnetization of γ-phase, $I_\gamma(T)$, on temperature, T, is characterized by $\partial I_\gamma/\partial T<0$ and $\partial^2 I_\gamma/\partial T^2 \geqq 0$, as exemplified in Fig. A-1. This general tendency of thermomagnetic curve of $I_\gamma(T)$ suggests that the distribution spectrum of Ni-content in γ-phase consists of a high concentration band of less than 30%Ni and a continuous spectrum of Ni-content which sharply decreases with an increase of Ni-content above 30%Ni.

The Ni-content in γ-phase being denoted by ξ, then, magnetization of γ-phase at T may be represented by

$$I_\gamma(T)=\int_{\xi_1}^{\xi_2} f(\xi) I_\gamma^\circ(\xi, T)d\xi, \tag{4}$$

where $f(\xi)$ and $I_\gamma^\circ(\xi, T)$ denote respectively the distribution spectrum of Ni-content and saturation magnetization of γ-phase of ξ in nickel content at T. There should be the lower and upper limits for the distribution of ξ, *i.e.* ξ_1 and ξ_2, in actual γ-phase grains in chondrites. As for $I_\gamma^\circ(\xi, T)$, BOZORTH's data (1951) can be adopted for $\xi \gtrsim 30\%$, but no reliable experimental data are available for $\xi<30\%$. As for Curie point (Θ_c) of γ-phase of Fe–Ni alloys, however, experimentally measured values are available for $\xi \gtrsim 25\%$. Referring to the thermomagnetic curves of Fe–Ni alloys for $\xi \gtrsim 30\%$, those for $\xi<30\%$ also would be approximately

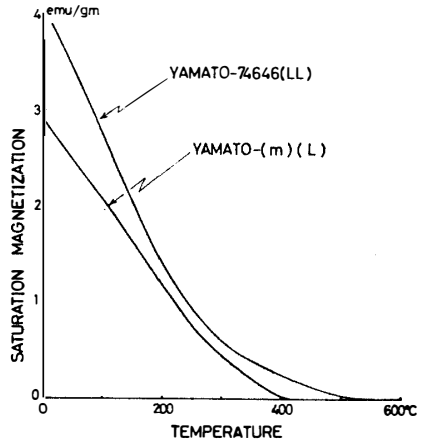

Fig. A-1. Examples of observed thermomagnetic curve of γ-phase.

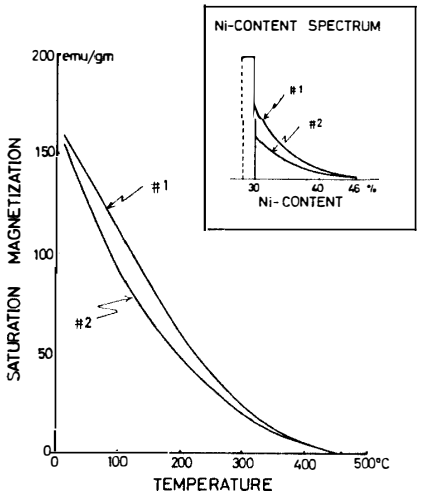

Fig. A-2. Thermomagnetic curves of model γ-phase. Model No. 1. Thermomagnetic curve of Model No. 1 of Ni-content spectrum. Model No. 2. Thermomagnetic curve of Model No. 2 of Ni-conent spectrum.

expressed by $I_\gamma°(\xi, T)=I_\gamma°(\xi, 0)\,[1-(T/\Theta_c)^n]^{1/n}$, where $n\simeq 3$. As $I_\gamma°(\xi, 0)$ values are reasonably well known, $I_\gamma(T)$ can be approximately evaluated with the aid of eq. (4), if the functional form of $f(\xi)$ is appropriately assumed.

On the basis of knowledge of the M-shape distribution of Ni-content in the taenite bands in iron meteorites as well as the lattice diffusion theory of Ni atoms through the *fcc* crystal structure of taenite phase, it is almost certain that a larger part of γ-phase in meteorites is represented by a sharp band spectrum of a range of 25–30 wt%Ni and a continuous Ni-content spectrum expressed by a form of $\exp(-k^2\xi)$ for a range of $\xi>30\%$. Assuming various numerical forms of $f(\xi)$ on these probable conditions, $I_\gamma(T)$ is calculated as a function of T with the aid of eq. (4) to fit the observed $I(T)\sim T$ curve. Among a number of numerically estimated curves for the $I(T)\sim T$ relation, it seems that Model No. 1 illustrated in Fig. A-2 is reasonably fit for the observed curve for H- and L-chondrites. The assumed spectrum of Ni-content distribution for Model No. 1 is illustrated in Fig. A-2, together with that for Model No, 2 and the resultant $I°(T)\sim T$ curve for Model No, 2, where the relative abundance of component of 30% in Model No, 2 is considerably less than that in Model No. 1.

The average value of ξ is 30.9 and 29.7%, and $I_\gamma(T=20°C)$ value is 154 and 150 emu/gm for Model No. 1 and No. 2 respectively. Since Model No. 1 can approximately represent the general tendency of thermomagnetic curve of γ-phase in H- and L-chondrites, this model is adopted for the magnetic analysis of Yamato (j) and (m) chondrites in the present study. In the case of LL-chondrites, however, another model of γ-phase composition should be considered, because m(Ni)/[m(Fe) $+m$(Ni)] in the metallic phase in LL-chondrites is much larger than that in H- and L-chondrites and consequently the apparent Curie point of γ-phase is much higher in the former than in the latter, as illustrated in Fig. A-1.